

Interferometric selection of frequency comb modes

C. Perrella · P. S. Light · J. D. Anstie ·
F. N. Baynes · A. N. Luiten

Received: 12 October 2012 / Accepted: 25 April 2013 / Published online: 23 May 2013
© Springer-Verlag Berlin Heidelberg 2013

Abstract We demonstrate a scheme to split an optical frequency comb into four separate frequency combs, each with four times the repetition rate of the original, but which are offset in frequency from each other. These spectrally rarified “daughter” combs are generated using fibre interferometers that are actively stabilised. We describe how these “daughter” combs can be used to resolve ambiguities that occur when comparing an arbitrary frequency continuous-wave signal against an optical frequency comb.

1 Introduction

Researchers have long dreamed of optical domain versions of coherent instrumentation such as the frequency synthesiser, arbitrary waveform generator, or network analyser. The optical frequency comb has been the breakthrough that has brought this dream close to reality, and one already sees important applications in high precision laser spectroscopy [1–3], frequency metrology [4–7] and arbitrary waveform generation [8, 9].

Nonetheless, the frequency comb remains a complex tool that is yet to be incorporated into widely available coherent instrumentation. To use the comb in this type of

instrumentation requires three separate, but equally critical characteristics: (a) a compact and reliable comb source; (b) an inter-mode frequency spacing that is sufficiently high [10, 11] to identify each mode through conventional techniques [4], though not so high as to require extremely fast photonic techniques [12]; and (c) the means to unambiguously identify the difference in frequency between some arbitrary cw laser signal and the known comb mode frequencies [13, 14].

To meet requirement (a), the focus has been on fibre-based mode-locked lasers [15] and microresonators [16, 17]. Unfortunately, the mode spacing of conventional fibre-based mode-locked lasers is too narrow (100–250 MHz) to easily meet requirement (b) and hence, a number of attempts have been made to increase this spacing by either modifying the laser itself [11, 18], or manipulating the pulse stream [19–25]. One sees that a simple mixing of a raw frequency comb and a cw laser source (i.e. the conventional technique to ascertain frequency differences between two cw laser signals) does not satisfy requirement (c) as this approach yield ambiguous results in certain circumstances. For example, when the cw laser has a frequency that matches a comb mode, or falls midway between two comb lines, then the standard frequency comparison process yields zero-frequency or near-degenerate mixing products [13, 14]. The low repetition rate of modern fibre-based mode-locked lasers exacerbates this problem as these “dead zones” are relatively closely spaced in frequency (50–125 MHz).

Many different techniques have been proposed to circumvent this ambiguity problem. For example, one can isolate a single comb mode and then generate a beat note between the cw signal and this isolated mode [26, 27]. The inherent challenge with this type of approach is the requirement to automatically isolate a comb mode that is

C. Perrella · P. S. Light · J. D. Anstie · F. N. Baynes ·
A. N. Luiten (✉)
School of Physics, University of Western Australia, Crawley,
WA 6009, Australia
e-mail: andre.luiten@adelaide.edu.au

Present Address:

C. Perrella · P. S. Light · J. D. Anstie · A. N. Luiten
Institute for Photonics and Advanced Sensing (IPAS) and the
School of Chemistry and Physics, The University of Adelaide,
Adelaide, SA 5005, Australia

sufficiently close to the optical cw signal. Alternatively, one could re-tune or step the comb [13, 28] to avoid entering a dead zone, however, there is unavoidable loss of phase during these switching events [14]. In addition, this approach is not amenable to situations in which multiple simultaneous measurements are performed using a single comb. The more general solution to this problem falls into two classes: either an elegant dual-comb solution [29] where a vernier approach provides the required unambiguous information, or the use of auxiliary signals at a known frequency offset from the incoming signal [14]. By the right choice of repetition rate difference between the two combs, or of the offset frequency of these auxiliary signals, it is possible to guarantee an unambiguous beat note over a wide range in input signal frequency [14, 29]. In contrast to those approaches, here, we make use of just a single comb and slice it into four constituent combs—each with a repetition rate four times the original, but where each “daughter” comb is offset from the other by the original repetition rate. As we will show below, this allows us to unambiguously derive the frequency relationship between the incoming signal and the original reference comb. In this article, we demonstrate this by developing a scheme that automatically stabilises the required interferometric elements in the correct phase. We also consider the effect of errors in the interferometer delays on the resulting modified optical combs. It is important to note that here, we are demonstrating more than just repetition rate multiplication—we are modifying the optical spectrum itself to generate a sparser optical frequency comb. It is this aspect which requires careful phase stabilisation and which would not be necessary if the objective was merely to multiply the repetition rate.

2 Theory

A frequency comb can be expressed in the form: $E(\omega) = \sum_m \tilde{a}_m \delta(\omega - m\omega_r - \omega_o)$ where $\delta(x)$ is a Dirac delta function, ω_r is the repetition rate frequency, m is the mode number, ω_o is the carrier-envelope offset frequency, and where \tilde{a}_m represents the spectral phase and amplitude of the m th mode. For definiteness, let us consider the case where $\tilde{a}_m = \exp(-(\omega - \omega_c)^2 / (4\Delta\omega^2)) \exp(-is(\omega - \omega_c))$, which represents a Gaussian amplitude envelope centred at a frequency of ω_c , with an e-fold width of $\Delta\omega$ and which has allowed for a linear phase ramp with a slope of s . For a comb consisting of a large number of frequency modes (i.e. m has a large range), the corresponding time-domain representation is a train of pulses with a Gaussian pulse envelope:

$$E(t) \propto \sum_n \exp\left[-(t - nt_r - s)^2 / \tau^2\right] \exp[i(\omega_c t + \phi_{o,n})] \quad (1)$$

where $\tau = 1/\Delta\omega$ is the pulse duration, $t_r = 2\pi/\omega_r$ is the inter-pulse time, s sets a time offset of the pulse peak, and $\phi_{o,n} = n\omega_o t_r$ is the carrier phase offset for the n th pulse.

A standard approach to double the repetition rate of frequency combs [19, 23, 25, 30] is to inject the pulse train into an unbalanced Mach-Zehnder interferometer (MZI) where one arm of the MZI is designed to deliver a delay, τ_d , that is close to an odd multiple of $t_r/2$ with respect to the other arm (as shown in the first box on the left hand side of Fig. 1). As we will show, in general, this approach does not automatically double the inter-mode spacing of the comb. The pulse train at one of the output ports of the MZI can be written as $\text{MZI}(t) = E(t) + BE(t - \tau_d) \exp(i\psi)$ where B allows for inequality in the power of the two recombined combs, and $|\psi| < \pi$ accounts for the relative carrier phase (i.e. evaluated at ω_c) of the two recombined pulse trains at the output of the recombining beamsplitter. This phase difference ψ is set by the relative path length difference of the arms as well as the phase conditions at the input and output beamsplitters. We have chosen to express the recombined output in this way, splitting the time delay, τ_d , that sets the location of the pulse envelope, from the rapidly varying optical phase component, ψ , as this allows us to emphasise the key differences between modifying the pulse rate and modifying the spectrum of the comb.

If the output of this unbalanced MZI is detected with a fast photodetector (as is standardly done to generate a microwave comb [19, 23, 25, 30]), then we would detect a series of current pulses corresponding to the impulse response of the photodiode (because the optical pulse duration is much shorter than the detector response time). For an ideal photodetector, characterised by a simple response time of τ_{PD} , the power spectral density of the detector output will be $|\text{PD}(\omega)|^2 \propto \sum_m \tilde{b}_m \delta(\omega - m\omega_r)$ where

$$\tilde{b}_m = (1 + B^2 + 2B \cos[m\tau_d \omega_r]) \left(\frac{1}{4(1 + [m\omega_r \tau_{PD}]^2)} \right) \quad (2)$$

We note that this expression is independent of ψ and ω_o , and we further see that if $B \sim 1$ and $\tau_d \sim (n + \frac{1}{2})t_r$ (where $n \in \mathbb{Z}$), then the even harmonics of the repetition rate will be enhanced while the odd harmonics are suppressed—effectively the pulse repetition rate of the comb has been doubled. The independence of the result in Eq. 2 on the relative carrier phase, ψ , shows why it has been unnecessary to stabilise ψ in prior work aimed at repetition rate multiplication [19, 23, 25, 30].

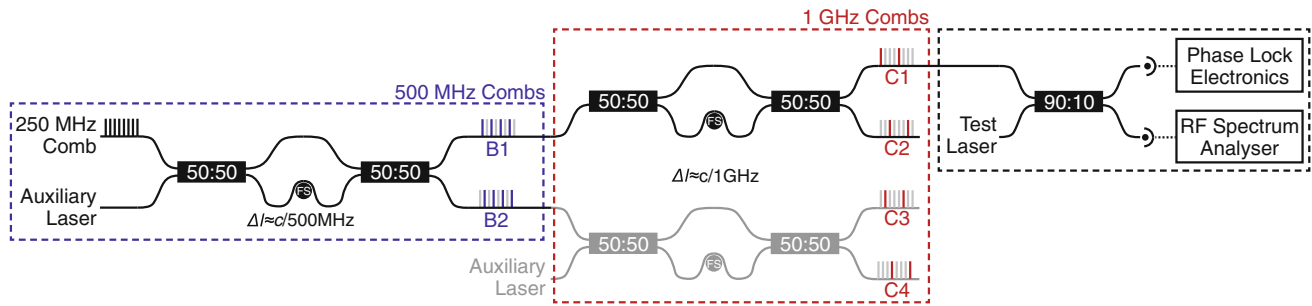


Fig. 1 The cascaded MZI setup used to achieve pulse rate multiplication, the phase monitoring components and frequency comparison stages is also shown. At each output, the remaining comb members are *highlighted*, and the original comb is shown in *grey*. *FS* fibre stretcher

In contrast, it is crucial to note that the *optical* spectrum of the interferometer output is sensitive to ψ . The power spectral density of $MZI(t)$ is proportional to

$$\sum_m \tilde{c}_m \delta(\omega - m\omega_r - \omega_o) \exp\left(-\tau^2(m\omega_r - \omega_c)^2\right) \quad (3)$$

where $\tilde{c}_m = 1 + B^2 + 2B \cos[\psi + \tau_d(m\omega_r - \omega_c)]$. From an examination of Eq. 3, it is clear that to split the original comb into odd- and even-mode combs, with each separately exiting from one of the ports of the MZI, it will be necessary to set power balance between the two combined combs ($B \sim 1$) while \tilde{c}_m must equal 0 for either odd or even m . It is clear that this only occurs when both $\tau_d \sim (n + \frac{1}{2})t_r$ for $n \in \mathbb{Z}$ and

$$\psi = \pi \frac{([2n + 1]\omega_c) \bmod \omega_r}{\omega_r}. \quad (4)$$

To explain more completely the effect of ψ , let us consider the simple case in which $\tau_d = \frac{t_r}{2}$ and where ω_c is an exact multiple of ω_r (i.e. $\omega_o = 0$). Let us then set ψ to be equal to zero as it must be according to Eq. 4. If we examine the time-domain behaviour of the output pulse train at B1, then we see that the output contains pulses delivered alternately from the upper and lower paths of the interferometer; however, the carrier phase of each output pulse is exactly the same (because $\psi = 0$). From the frequency domain view, this output comb has an inter-mode spacing of $2\omega_r$ with an ω_o of zero, that is, it is the even mode in the original input comb. If one examines the pulse stream at the B2 output (under the same circumstances), we note that the apparent carrier phase would be flipping by π between adjacent pulses (this is enforced by the phase relations of a beamsplitter [32]). One thus sees the B2 output comb as having an inter-mode spacing of $2\omega_r$ with an offset frequency, ω_o , equal to ω_r (i.e. exactly half the repetition rate of the output comb): this clearly corresponds to the odd modes of the input comb. We note also that this theory predicts a rather paradoxical situation: if ψ is not set to one of the special values in Eq. 4, then the output comb will contain energy from all modes in the original comb (i.e. a

mode spacing of ω_r) although the measured inter-pulse time would be $t_r/2$ rather than the expected t_r .

If there is an overall error in the interferometer arm imbalance, that is, $\tau_d = (n + \frac{1}{2})t_r + \Delta$ where Δ represents the time error, then there is a resulting effect on both the spectrum of the pulses as well as on the optical spectrum. The pulse repetition rate spectrum will only show the desired suppression of the odd harmonics with respect to the even harmonics for modes up to an RF frequency of $1/(4\Delta)$. In the optical spectrum, we will only obtain a splitting of odd and even modes over a limited range of the spectrum even if the value of ψ is held stable. The full frequency distance between the places where the odd and even comb modes becomes equal in amplitude (i.e. an estimate of the spectral distance over which the splitting is functional) is $1/(2\Delta)$. We demonstrate both of these effects experimentally. Further, we note that this technique is reasonably broadband since an arm length error of $10 \mu\text{m}$ can still lead to a bandwidth of 15 THz.

3 Experiment

The original comb is generated by a commercial 250 MHz repetition rate fibre mode-locked laser, which is frequency-doubled to 780 nm. The comb is injected into two cascaded fibre-based MZIs as shown in Fig. 1. The phase imbalance, ψ , in each MZI is detected by injecting a cw auxiliary signal into the input of the first stage and then modulating fibre stretchers that are placed in one arm of each of the two MZIs. The fibre stretchers are modulated at different frequencies (~ 2.5 and 3 kHz) resulting in dual synchronous modulation of the output power at the output of the second MZI. This signal is detected with two lock-in amplifiers to generate independent error signals, which are used to stabilise the relative phase, ψ , in both MZIs using the stretchers. No synchronous power modulation arises from the presence of the comb in the MZIs as there is no optical interference when the two time-displaced combs are recombined.

The output of the lockin amplifiers is zero when the auxiliary laser is in constructive or destructive interference at the monitored port. By tuning the frequency of the auxiliary laser, we can stabilise ψ at any arbitrary value. To demonstrate the efficacy of the ψ locking system, the output of the first MZI stage was coupled to both an optical cavity and a fast photodiode (see Fig. 2). The optical cavity has a free-spectral range of 29.4 GHz with a finesse of ~ 300 . We used a monochromator to filter out ~ 30 GHz of the spectrum to prevent the confusion of overlapping cavity orders (although small overlaps are still visible at the extrema of Fig. 2a). It is the filtering effect of the monochromator that is responsible for the overall envelope of the optical comb seen in the top panel of Fig. 2a—the actual comb itself is much broader than that displayed. The output from the optical cavity as it is scanned is shown in Fig. 2a while Fig. 2b shows the spectrum at the output of the fast photodiode detecting that optical comb. In the first row, we have adjusted the arm imbalance to the optimal value (i.e. $\Delta = 0$), while across the two lower rows, we have intentionally maladjusted the MZI by inserting free-space elements of 15 and 29 mm, respectively, into one arm ($\Delta = \Delta l/c \sim 5, 10 \times 10^{-11}$).

As predicted, the photodiode output spectra (i.e. Fig. 2b) were seen to be independent of the value of ψ , that is, the spectra shown in Fig. 2b were stable in time and did not vary if ψ was intentionally varied. In contrast, the optical spectrum viewed from one output port was seen to evolve from a purely odd through to a even mode comb if ψ was not actively stabilised. However, if one locks ψ to a particular value, then the interferometer can stably deliver either the even (or odd) modes of the input frequency comb to output port B1.

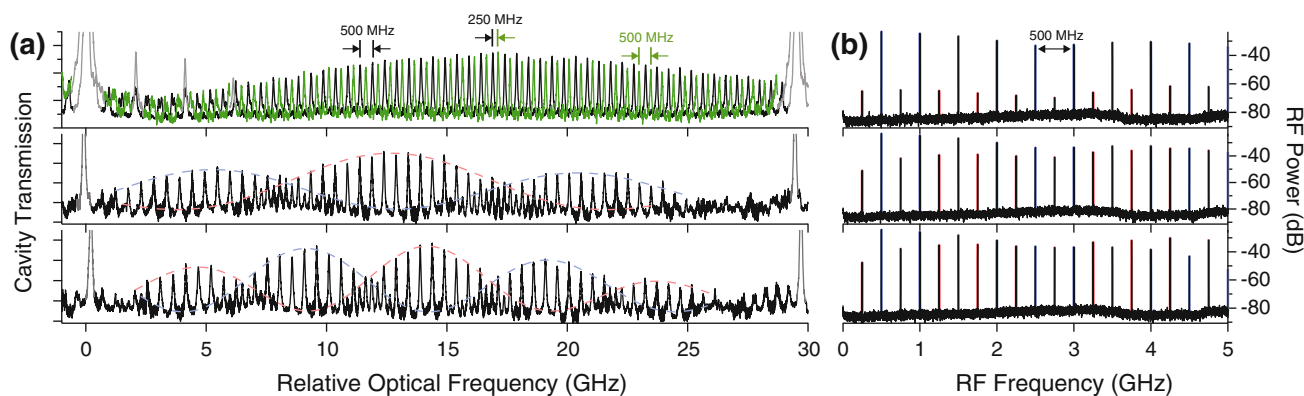


Fig. 2 Measured optical spectra (a) and microwave spectra (b) at the output of a single MZI stage. The microwave comb is generated by detecting the optical comb with a photodiode while the optical comb is measured by its transmission through a high-resolution optical cavity (linear transmission units). *Top panel* is the output of a MZI with optimally set arm length imbalance ($\Delta \sim 0$ s) and $\psi = 0$ at position B1 (black) and B2 (green) with a 500 MHz repetition rate; *Middle panel* inserted a 15 mm free-space section to imbalance the

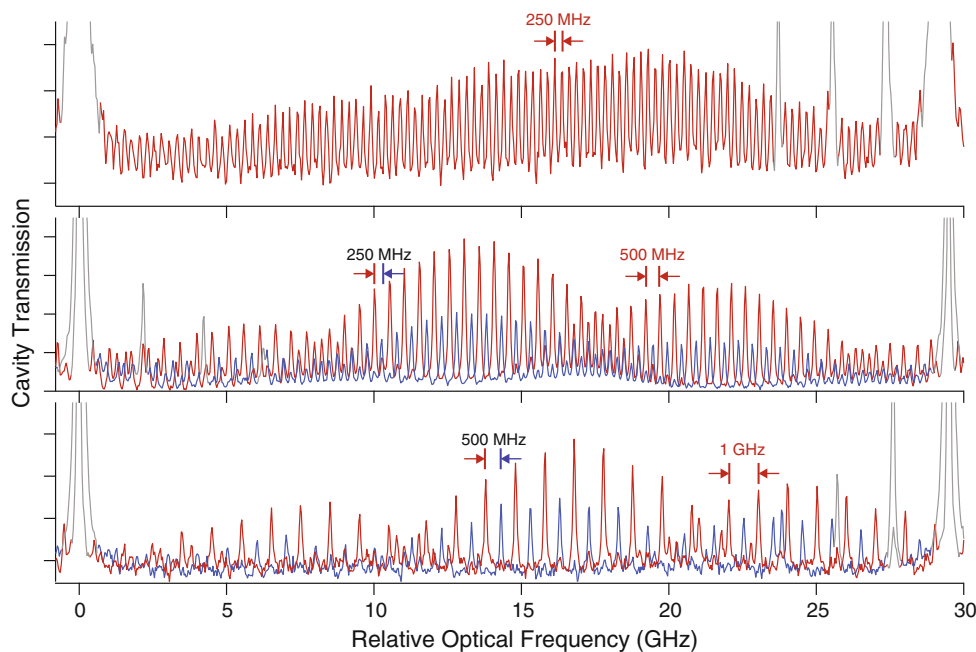
interferometer ($\Delta \sim 5 \times 10^{-11}$ s); *Bottom panel* inserted 29 mm free-space section ($\Delta \sim 9.7 \times 10^{-11}$ s). The grey peaks on the optical spectra are auxiliary cw lasers marking a free-spectral range of the optical cavity. The dashed blue and red envelopes on the optical spectrum serve as a guide to the eye. The red and blue background on the photodiode spectra mark the odd and even ω_r harmonics, respectively

The lower two rows of Fig. 2 demonstrate the effect of maladjustment of the gross arm imbalance on the optical and microwave combs. Using the expressions given earlier, we predict that the suppression of the 250 MHz peaks on the microwave comb with respect to the 500 MHz peaks will disappear at an RF frequency of 5 and 2.6 GHz, respectively, for the presented arm imbalances. This is in good agreement with the measured values of ~ 4.5 and ~ 2.5 GHz derived from Fig. 2b.

The optical spectrum shows corresponding behaviour for these gross time delay errors: we see the production of side-lobes surrounding the central lobe where the output modes have the opposite parity to those in the central lobe. Once again, the experimental data support the analysis by showing a central lobe full width of 8.9 and 5.1 GHz respectively, which is in reasonable agreement with expected values of 10 and 5.2 GHz.

In Fig. 3, we show the measured optical spectrum of the comb through multiple MZI stages: the top panel displays the unmodified raw comb where we are just able to resolve the 250 MHz fundamental comb spacing. Once again the overall comb envelope seen here is associated with the monochromator filter (to prevent multiple order spectra from overlapping in the output) and is not a feature of the comb-splitting technique. In the middle panel, we observe the two outputs of the first stabilised MZI stage with 500 MHz comb spacing (positions B1 and B2 as red and blue respectively on Fig. 1). On the bottom panel, we display the two outputs from the second MZI stage with 1 GHz comb spacing (positions C1 and C2 as red and blue, respectively, on Fig. 1). Here, as on Fig. 2, one sees the effect of an error in the interferometer arm imbalances, which causes the modulation of the comb envelope as well

Fig. 3 Optical spectrum measured in transmission through the detection optical cavity (linear relative transmission). *Top* Direct comb output (250 MHz Rep. Rate). The amplitude modulation across the comb in the upper panel is a result of the monochromator filter in the detection; *Middle* Output of first stage (500 MHz Rep. Rate); *Bottom* Output after two MZI stages (1 GHz Rep. Rate). The red and blue curves show the output of the two output ports of the relevant stage. The modulation and the switching of odd and even peaks in the lobes seen in the lower panels arises from an error in the selected arm length imbalance. The peaks from the auxiliary laser have been coloured light grey



as the switching of the odd and even harmonics between the two output ports. Nonetheless, the suppression of the unwanted modes exceeded 12 dB for this set-up—we were unable to measure the full suppression because of the noise floor of the measurement. By careful adjustment of the lengths of the arms (as shown in [22, 23]), it is possible to suppress this modulation. The outputs from the parallel second-stage MZI (positions C3 and C4 on Fig. 1) are offset by 250 MHz from those seen at C1 and C2.

To rotate ψ through one full cycle (2π), it is necessary to tune the auxiliary laser frequency by one inter-mode spacing as measured at the output of the last interferometer stage (i.e. 1 GHz in our demonstration system). The frequency stability of the auxiliary laser in our case was around 10 MHz which was sufficient to maintain a stable comb output from one of the interferometer ports—we calculate that a 10 MHz error in the setting of this auxiliary laser frequency still allows more than 30 dB of suppression of the unwanted modes of the comb. If higher suppression is necessary, then it is possible to offset frequency lock [31] the auxiliary laser to one of the comb modes giving the approach indefinite stability.

Finally, to demonstrate the effectiveness of our approach, we combined the output of the MZI-cascade with a continuous-wave (cw) laser to generate a heterodyne mixing signal (as shown on Fig. 1). This is displayed on Fig. 4 as a two-dimensional intensity plot where the darkness of a pixel represents the strength of the corresponding Fourier frequency. The five vertical lines on the two plots represent the repetition rate signals for the raw comb (upper panel) and the output of the two cascaded MZI stages. One notes that on the lower panel that the

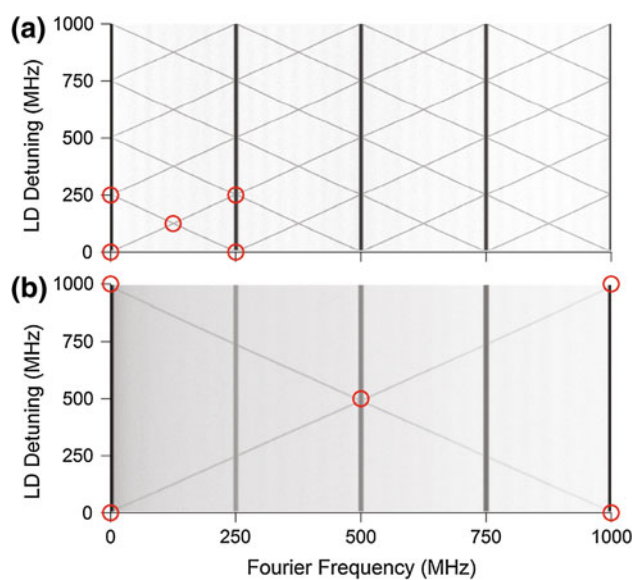


Fig. 4 Two-dimensional intensity plot of a CW laser beat note with **a** the raw comb and **b** the output of the two cascaded MZI stages, that is, the divided comb, as the CW laser frequency is scanned (vertical axis). The red circles represent areas where the beat note becomes ambiguous

1 GHz peak is now much stronger than the 250, 500 and 750 MHz signals as a result of the filtering of the cascaded MZIs. As the frequency of the cw laser is scanned (vertical axis), we see multiple beat notes due to the mixing products between the laser and the various modes of the combs. The red circles show areas where the beat note coalesces when $f_{\text{las}} - mf_r + f_0 \sim nf_r/2$ (for $n \in \mathbb{Z}$). It is in these places where a simple frequency measurement of the difference frequency between the comb and cw laser cannot

easily yield the frequency of the cw laser. It is clear that this situation occurs 4 times less frequently in the rarified optical comb. However, much more important than that simple observation is the fact that our scheme gives us the means to completely avoid any of these degenerate or zero-frequency beat notes. If we observe the beat note between the comb and the cw laser falling within $f_r/8$ of f_r , then we immediately flip the phase of ψ in the first stage by π . This can be done simply by moving the auxiliary laser signal. In this case, the output comb shifts in frequency by exactly $f_r/4$ yielding a new beat note that has a unique interpretation. An alternative technique, which can avoid the need for this switching, is the use of two parallel second-stage MZIs, as indicated in Fig. 1. In this case, all four daughter combs are available continuously at C1–C4, and one just chooses the particular mixing product that provides an unambiguous output.

4 Conclusion

We have demonstrated that phase-stabilised MZIs are capable of separating an optical frequency comb into odd and even modes and delivering these “daughter” combs at separate ports. We have cascaded two of these stages and developed a technique to actively stabilise the MZIs. This approach delivers four daughter combs that are all offset in frequency from each other. We have furthermore explicitly demonstrated the effect of arm length errors on the optical comb and its consequence for microwave combs generated from these pulse trains, and have demonstrated the ability to measure arbitrary frequency signals using these divided combs.

Acknowledgments We would like to thank the Australian Research Council for supporting this research under the Grants DP0877938, FT0991631 and DP1094500.

References

1. R. Holzwarth, T. Udem, T. Hansch, J. Knight, W. Wadsworth, P. Russell, Optical frequency synthesiser for precision spectroscopy. *Phys. Rev. Lett.* **85**, 2264–2267 (2000)
2. M.J. Thorpe, K.D. Moll, R.J. Jones, B. Safdi, J. Ye, Broadband cavity ringdown spectroscopy for sensitive and rapid molecular detection. *Science* **311**, 1595–1599 (2006)
3. S.A. Diddams, L. Hollberg, V. Mbele, Molecular fingerprinting with the resolved modes of a femtosecond laser frequency comb. *Nature* **445**, 627–630 (2007)
4. T. Udem, R. Holzwarth, T.W. Hänsch, Optical frequency metrology. *Nature* **416**, 233–237 (2002)
5. L.-S. Ma, Z. Bi, A. Bartels, L. Robertsson, M. Zucco, R.S. Windeler, G. Wilpers, C. Oates, L. Hollberg, S.A. Diddams, Optical frequency synthesis and comparison with uncertainty at the 10^{-19} level. *Science* **303**, 1843–1845 (2004)
6. S.A. Diddams, T. Udem, J.C. Bergquist, E.A. Curtis, R.E. Drullinger, L. Hollberg, W.M. Itano, W.D. Lee, C.W. Oates, K.R. Vogel, D.J. Wineland, An optical clock based on a single trapped 199Hg^+ ion. *Sci. Agric.* **293**, 825–828 (2001)
7. H.S. Margolis, G.P. Barwood, G. Huang, H.A. Klein, S.N. Lea, K. Szymaniec, P. Gill, Hertz-level measurement of the optical clock frequency in a single 88Sr^+ ion. *Science* **306**, 1355–1358 (2004)
8. Z. Jiang, C.-B. Huang, D.E. Leaird, A.M. Weiner, Optical arbitrary waveform processing of more than 100 spectral comb lines. *Nat. Photonics* **1**, 463–467 (2007)
9. A.M. Weiner, Femtosecond pulse shaping using spatial light modulators. *Rev. Sci. Instrum.* **71**, 1929–1961 (2000)
10. M.S. Kirchner, D.A. Braje, T.M. Fortier, A.M. Weiner, L. Hollberg, S.A. Diddams, Generation of 20 GHz, sub-40 fs pulses at 960 nm via repetition-rate multiplication. *Opt. Lett.* **34**, 872–874 (2009)
11. A. Bartels, D. Heinecke, S.A. Diddams, 10-GHz self-referenced optical frequency comb. *Science* **326**, 681 (2009)
12. A.R. Johnson, Y. Okawachi, J.S. Levy, J. Cardenas, K. Saha, M. Lipson, A.L. Gaeta, Chip-based frequency combs with sub-100 GHz repetition rates. *Opt. Lett.* **37**, 875–877 (2012)
13. J. Jost, J. Hall, J. Ye, Continuously tunable, precise, single frequency optical signal generator. *Opt. Express* **10**, 515–520 (2002)
14. T.R. Schibli, K. Minoshima, E.L. Hong, H. Inaba, Y. Bitou, A. Onae, H. Matsumoto, Phase-locked widely tunable optical single-frequency generator based on a femtosecond comb. *Opt. Lett.* **30**, 2323–2325 (2005)
15. B. Washburn, S. Diddams, N. Newbury, J. Nicholson, M. Yan, C. Jorgensen, Phase-locked, erbium-fiber-laser-based frequency comb in the near infrared. *Opt. Lett.* **29**, 250–252 (2004)
16. P. Del’Haye, A. Schliesser, O. Arcizet, T. Wilken, R.T. Holzwarth, J. Kippenberg, Optical frequency comb generation from a monolithic microresonator. *Nature* **450**, 1214–1217 (2007)
17. T. Kippenberg, R. Holzwarth, S. Diddams, Microresonator-based optical frequency combs. *Science* **331**, 555–559 (2011)
18. D. Kielpinski, O. Gat, Phase-coherent repetition rate multiplication of a mode-locked laser from 40 MHz to 1 GHz by injection locking. *Opt. Express* **20**, 2717–2724 (2012)
19. S.A. Diddams, M.S. Kirchner, T. Fortier, D.A. Braje, A. M. Weiner, L. Hollberg, Improved signal-to-noise ratio of 10 GHz microwave signals generated with a mode-filtered femtosecond laser frequency comb. *Opt. Express* **17**, 3331–3340 (2009)
20. J. Chen, J.W. Sickler, P. Fendel, E.P. Ippen, F.X. Kärtner, T. Wilken, R. Holzwarth, T.W. Hänsch, Generation of low-timing-jitter femtosecond pulse trains with 2 GHz repetition rate via external repetition rate multiplication. *Opt. Lett.* **33**, 959–961 (2008)
21. M.T. Murphy, C.R. Locke, P.S. Light, A.N. Luiten, J.S. Lawrence, Laser frequency comb techniques for precise astronomical spectroscopy. *Mon. Not. R. Astron. Soc.* **422**, 761–771 (2012)
22. M.Y. Sander, S. Frolov, J. Shmulovich, E.P. Ippen, F.X. Kärtner, 10 GHz femtosecond pulse interleaver in planar waveguide technology. *Opt. Express* **20**, 4102–4113 (2012)
23. A. Haboucha, W. Zhang, T. Li, M. Lours, A.N. Luiten, Y. Le Coq, G. Santarelli, Optical-fiber pulse rate multiplier for ultralow phase-noise signal generation. *Opt. Lett.* **36**, 3654–3656 (2011)
24. S.-S. Min, Y. Zhao, S. Fleming, Repetition rate multiplication in figure-eight fibre laser with 3dB couplers. *Opt. Commun.* **277**, 411–413 (2007)
25. T. Fortier, M. Kirchner, F. Quinlan, J. Taylor, J. Bergquist, T. Rosenband, N. Lemke, A. Ludlow, Y. Jiang, C. Oates, S. Diddams, Generation of ultrastable microwaves via optical frequency division. *Nat. Photonics* **5**, 425–429 (2011)
26. H. Inaba, T. Ikegami, F.-L. Hong, A. Onae, Y. Koga, T. Schibli, K. Minoshima, H. Matsumoto, S. Yamadori, O. Tohyama, S.-I. Yamaguchi, Phase locking of a continuous-wave optical parametric oscillator to an optical frequency comb for

- optical frequency synthesis. *IEEE J. Quantum Elect.* **40**, 929–936 (2004)
27. Y.-J. Kim, Y. Kim, B.J. Chun, S. Hyun, S.-W. Kim, All-fiber-based optical frequency generation from an Er-doped fiber femtosecond laser. *Opt. Express* **17**, 10939–10945 (2009)
28. B. Washburn, R. Fox, N. Newbury, J. Nicholson, K. Feder, P. Westbrook, C. Jørgensen, Fiber-laser-based frequency comb with a tunable repetition rate. *Opt. Express* **12**, 4999–5004 (2004)
29. F.R. Giorgetta, I. Coddington, E. Baumann, W.C. Swann, N.R. Newbury, Fast high-resolution spectroscopy of dynamic continuous-wave laser sources. *Nat. Photonics* **4**, 853–857 (2010)
30. H. Jiang, J. Taylor, F. Quinlan, T. Fortier, S.A. Diddams, Noise floor reduction of an Er: fiber laser-based photonic microwave generator. *IEEE Photon. J.* **3**, 1004–1012 (2011)
31. H. Jiang, J. Taylor, F. Quinlan, T. Fortier, S. A. Diddams, Noise floor reduction of an Er: fiber laser-based photonic microwave generator. *IEEE Photon. J.* **3**, 1004–1012 (2011)
32. A. Seigman, *Lasers*. (University Science Books, Mill Valley, 1986)